

Modelling of atmospheric concentrations of fungal spores: a two-year simulation over France using CHIMERE.

Matthieu Vida¹, Gilles Foret², Guillaume Siour², Florian Couvidat³, Olivier Favez^{3,4}, Gaelle Uzu⁵, Arineh Cholakian⁶, Sébastien Conil⁷, Matthias Beekmann¹ and Jean-Luc Jaffrezo⁵.

¹Université Paris Cité and Univ Paris Est Creteil, CNRS, LISA, F-75013 Paris, France

²Univ Paris Est Creteil and Université Paris Cité, CNRS, LISA, F-94010 Créteil, France

³Institut National de l'Environnement Industriel et des Risques, INERIS, F-60550 Verneuil-en-Halatte, France

⁴Laboratoire Central de Surveillance de la Qualité de l'air, LCSQA, F-60550 Verneuil-en-Halatte, France

⁵Institut des Géosciences de l'Environnement, IGE, UGA, CNRS, IRD, G-INP, INRAE, F-38000 Grenoble, France

⁶Laboratoire de Météorologie Dynamique (LMD), Ecole Polytechnique, IPSL Research University, Ecole Normale Supérieure, Université Paris-Saclay, Sorbonne Universités, UPMC Université Paris 06, CNRS, Route de Saclay, F-91128 Palaiseau, France

⁷ANDRA DISTEC/EES Observatoire Pérenne de l'Environnement, F-55290, Bure, France

Correspondence: Gilles Foret (gilles.foret@lisa.ipsl.fr) & Gaelle Uzu (gaelle.uzu@ird.fr)

Abstract

Fungal spore organic aerosol emissions have been recognised as a significant source of particulate matter as PM₁₀; however, they are not widely considered in current air quality models. In this work, we have implemented the parameterisation of fungal spore organic aerosol (OA) emissions introduced by Heald and Spracklen (2009) (H&S) and further modified by Hoose et al. (2010) in the CHIMERE regional chemistry-transport model. This simple parameterisation is based on two variables, leaf area index (LAI) and specific humidity. We have validated the geographical and temporal representativeness of this parameterisation on a large scale by using yearly polyol observations and primary biogenic organic aerosol factors from PMF analysis at 11 French measurement sites. For a group of sites in northern and eastern France, the seasonal variation of fungal spore emissions, displaying large summer and small winter values, is correctly depicted. However, the H&S parameterisation fails to capture fungal spore concentrations for a smaller group of Mediterranean sites with less data availability both in terms of absolute values as well as seasonal variability, leading to strong negative biases especially during the autumn and winter seasons occur. Two years of CHIMERE simulations with the H&S parameterisation have shown a significant contribution of fungal spore OA to PM₁₀ mass, lower than 10 % during winter, and reaching up to 20 % during summer in high emission zones, especially over large forested areas. In terms of contribution to organic matter (OM) concentrations, the simulated fungal spore contribution in autumn is as high as 40 % and reaches at most 30 % of OM for other seasons. As a conclusion, the fungal spore OA contribution to total OM concentrations is shown to be substantial enough to be considered as a major PM₁₀ fraction and should then be included in state-of-the-art chemistry transport models.

1. Introduction

48
50
52
54
56
58
60
62
64
66
68
70
72
74
76
78
80
82
84
86
88
90
92
94

Modelling of the organic matter (OM) fraction of PM₁₀ with chemical transport models can be complex due to the varied composition of organic matter, which is not yet fully known, incomplete emission inventories or their inherent uncertainties, and poorly parameterised atmospheric chemical transformations.

It is therefore important to assess whether the primary source of organic aerosol, currently not considered in many models, can help to improve atmospheric aerosol modelling. Primary biogenic organic aerosols (PBOA) are mainly composed of microorganisms such as bacteria, fungi, fungal or bacterial spores, pollens or viruses and biological fragments such as plant debris or microbes (Després et al., 2012; Fröhlich-Nowoisky et al., 2016; Jaenicke et al., 2007). Their size varies from less than 0.3 µm for viruses to about 100 µm for pollens (Després et al., 2012; Jones and Harrison, 2004; Shaffer and Lighthart, 1997). When looking at atmospheric particles with an aerodynamic diameter of less than 2.5 or 10 µm (which are the fractions routinely measured and studied for health risk assessment), it is possible to find viruses, bacteria (agglomerated or not) and spores; however spores, when produced by fungi, represent the major fraction in terms of mass (Elbert et al., 2007).

More specifically, fungal spores are emitted directly into the atmosphere during the fungal reproduction process when temperature and humidity conditions are favourable, but their emission can also be triggered by wind and rain (Elbert et al., 2007; Huffman et al., 2013; Jones and Harrison, 2004). Previous studies estimated that fungal spores can contribute to around 5 % and 10 % of the mass of respectively PM₁₀ and organic carbon, in urban and suburban areas (Bauer et al., 2002, 2008b). In specific environments such as tropical forests, the contribution of fungal spores can represent 45 % of the PM₁₀ mass (Elbert et al., 2007).

Fungal spores are susceptible to cause major health problems such as asthma, pulmonary obstruction, tuberculosis, meningitis and legionellosis (Douwes et al., 2003; Eduard et al., 2012; Fröhlich-Nowoisky et al., 2016; Ghosh et al., 2015; Pearson et al., 2015; Samaké et al., 2017). Some studies on PBOA have shown that aerosols emitted directly by fungi in the form of spores contribute significantly to the oxidative potential of aerosols (Samaké et al., 2017). Moreover, based on a positive matrix factorisation (PMF) analysis, Weber et al. (2021) derived a primary biogenic factor based on a large data set of speciated PM₁₀ aerosol measurements over France, including polyol measurements as a tracer for fungal spores. They found a high intrinsic oxidative potential by dithiothreitol (DTT) for this factor, equal to that of biomass burning, but lower than that of primary traffic emissions.

Literature review shows several parameterisations suitable for use of modelling primary biogenic aerosols emissions from fungal spores in the PM₁₀ size range in chemistry transport models. Samaké et al. (2019a) identified the parameters responsible for up to 82 % of the annual variability of polyols as a tracer of fungal spores for a temperate latitude site in an alpine environment, using multi-linear approaches. These variations were mainly explained by the mean night-time temperature (54 %) and LAI (37 %), and to a lesser extent by the atmospheric humidity (3 %) and the wind speed (2 %). The combined factor of LAI and wind speed explains the remaining variability (4 %). A first parameterisation for the treatment of fungal scores in atmospheric models was proposed by Heald and Spracklen (2009) (H&S) and modified by Hoose et al. (2010). It estimates fungal spore emissions as a linear

96 function of leaf area index (LAI) and specific humidity. In this formulation, the LAI is a
97 proxy for the vegetation density and the specific humidity is a proxy for the water
98 availability, but is also related temperature. The parameterisation proposed by Sesartic
99 and Dallafior (2011) (S&D) suggests a different approach by varying emissions as a
100 function of soil types, not relying on LAI, and therefore removing the seasonality
101 inherently present in the H&S parameterisation. Hummel et al. (2015) compared these
102 parameterisations across Europe and developed a new statistical model, based on the
103 H&S parameterisation using LAI and specific humidity, to also include a linear
104 dependence with temperature, and a threshold below which emissions are assumed
to be zero.

106 In Hummel et al. (2015), the concentrations simulated with three
107 parameterisations of H&S, S&D and Hummel were compared to measurements of
108 fluorescent biological aerosol particles (FBAP) at four sites in several parts of Europe
109 (Germany, Finland, UK, Ireland) for almost weekly time periods in July, August and
110 October of 2010. This comparison was carried out using 1,536 hourly data points, that
111 most of which came from the German (600) and Finnish (600) stations. At these two
112 sites, one week in July, one week in August and 10 days in September were measured,
113 unlike the UK and Irish sites, where the data was taken only for August 2010. FBAP
114 measurements are taken as a proxy for fungal spore emissions. By construction, the
115 S&D parameterisation does not reproduce the observed daily and seasonal variability,
116 while it is known that fungal spore emissions display a general summer maximum
117 across Europe (Samaké et al., 2019a, b). On the contrary, the H&S and Hummel
118 parameterisations include these temporal variations and therefore show better
119 correlations with measured concentrations ($R = 0.43$) compared to the S&D approach
120 ($R = -0.05$). The parameterisation by Hummel et al. (2015) showed a lower normalised
121 mean bias (NMB = -43 %) compared to the H&S one (NMB = -44 %).

122
123 As fungal spores make a significant contribution to PM_{10} and are rarely included
124 in chemistry transport models (CTM), the aim of our study is to integrate them into the
125 state-of-the-art Chemistry Transport Model CHIMERE (Menuet et al., 2021), to evaluate
126 the model performance with field measurements, and to infer the spatio-temporal
127 variability of their occurrence. This could lead to improved modelling of PM_{10}
128 concentrations, of organic matter, and of other pollutants such as secondary biogenic
129 compounds or even oxidative potential. This study will focus on France, displaying one
130 of the largest database of chemically speciated PM measurements in Europe (Favez
131 et al., 2021). Interestingly, France has a wide range of climatic variability (oceanic,
132 semi-oceanic, continental, mountainous, Mediterranean), making it possible to
133 compare fungal spore modelling results under various climatic conditions. To assess
134 the modelling of fungal spores, measurements of polyols were used, specifically
135 mannitol and arabitol, since many studies indicate that they are specific tracers of this
136 PBOA fraction (Bauer et al., 2008a; Gosselin et al., 2016; Samaké et al., 2019a).
137 Furthermore, we compared our CTM results to the concentrations of organic matter
138 ascribed to this primary biogenic source using the receptor model Positive Matrix
139 Factorisation (PMF) in previous work.

140

2. Material & methods

142 2.1. Observations

144 2.1.1. PM₁₀ and Organic matter measurements

146 The PM₁₀ mass concentration data have been obtained from continuous
148 measurements performed by French regional air quality monitoring networks (AQMN).
150 These observations have been achieved by AQMN using two types of automated
152 analysers during this period: tapered element oscillating microbalances equipped with
154 filter dynamic measurement systems (TEOM-FDMS, Thermo Scientific), and beta
156 radiation absorption analysers (Met One BAM 1020 and ENVEA MP101M). These
158 measurements have been conducted in accordance with standard procedures
160 described in CSN EN 16450. As described by Favez et al. (2021), the aim of the
162 aerosol characterisation program (CARA) is to develop knowledge of the chemical
164 composition and contribution of atmospheric particle sources. This work is enriched by
research programmes, with data from some of them being used in this study. In CARA
and other programs, the chemical analysis of (PM₁₀) filter samples has been performed
following relevant European standard methods. Briefly, for datasets used herein,
organic carbon was measured by thermo-optical analysis using the EUSAAR2 protocol
(Cavalli et al., 2010). Sugars were measured by liquid chromatography using pulsed
amperometric detection (Verlhac et al., 2013; Yttri et al., 2015). The measurement
protocols have been detailed in previous studies (Samaké et al., 2017, 2019a, b;
Weber et al., 2021). The analysed species include mannitol and arabitol, which
currently make up for a large fraction of organic sugars (Elbert et al., 2007) and are
used as a tracer for fungal spore emissions.

166 In summary, for the datasets used in the present study, PM₁₀ organic matter
168 observations were performed at 13 different stations for a total of 2,227 daily filter
170 samples, including 1,497 data on polyols on 11 sites. The locations of these sites are
illustrated in Figure 1, while Table 1 provides details on the number of data points
available per station and their temporality.

172 2.1.2. OC apportionment based on filter samples

174 Positive Matrix Factorisation (PMF) is one of the most widely used techniques
176 for identifying factors contributing to aerosol concentrations using online and offline
178 measurement data (Belis et al., 2020; Hopke et al., 2020; Karagulian et al., 2015;
180 Paatero and Tapper, 1994). This receptor model commonly uses off-line chemical
182 speciation measured on filters and factor-specific tracers as input data. The correlation
184 matrices allow the identification of the species co-emitted with the tracers and thus
186 determine the contribution of the factors to the PM₁₀ concentrations. For this study,
188 PMF analysis were previously performed with a harmonised methodology (Weber et
al., 2021), providing source apportionment results for a total number of 842 daily data
at 7 french sites from early 2013 to the end of 2014. PMF results at all sites include a
factor which can be attributed to PBOA because of the large concentrations of the two
polyols in this factor, representing more than 90 % of the polyols total mass in this
factor (Samaké et al., 2019a). The organic carbon of the primary biogenic PMF was
multiplied by a factor of 1.8 to obtain the organic matter concentrations of this PMF
factor (OMpb) (Favez et al., 2010; Petit et al., 2015). However, this PBOA factor may
also contain biogenic secondary organic aerosols (BSOA) since it is sometimes

190 associated with BSOA tracers, such as 3-MBTCA (resulting from α -pinene oxidation)
 191 or 2-MTs (resulting from oxidation of isoprene) (Borlaza et al., 2021). Therefore, we
 192 propose here to use the PBOA factor as an upper boundary for fungal spore
 concentrations (see section 3.2).

194

196 **Table 1 : Summary of the number of daily filters analysed for polyols as well as OM from primary biogenic
 197 factor derived from PMF analysis (OMpb) available for this study over the years 2013 and 2014 at different
 198 French sites (within the PM₁₀ fraction). The measurement period and geographical coordinates (latitude ;
 longitude ; altitude) are also indicated.**

Stations	Coordinates (lat ; lon ; alt)	Measurement period	OMpb	Polyols
Aix-en-Provence	43.53 ; 5.44 ; 192 m	18.07.2013 – 13.07.2014	56	117
Andra-OPE	48.55 ; 5.46 ; 386 m	01.01.2013 – 29.12.2014	/	98
Grenoble	45.16 ; 5.74 ; 219 m	02.01.2013 – 29.12.2014	237	238
Lens	50.44 ; 2.83 ; 47 m	05.04.2013 – 26.09.2014	167	138
Marseille	43.30 ; 5.39 ; 73 m	01.06.2014 – 31.12.2014	/	95
Nice	43.70 ; 7.29 ; 11 m	04.06.2014 – 31.12.2014	77	89
Nogent-sur-Oise	49.28 ; 2.48 ; 28 m	02.01.2013 – 31.12.2014	155	220
Port-de-Bouc	43.40 ; 4.98 ; 3 m	01.06.2014 – 31.12.2014	79	80
Revin	49.91 ; 4.63 ; 394 m	02.01.2013 – 26.09.2014	/	168
Roubaix	50.71 ; 3.18 ; 31 m	20.01.2013 – 08.09.2014	/	159
Strasbourg	48.59 ; 7.74 ; 139 m	02.04.2013 – 31.12.2014	71	95

200

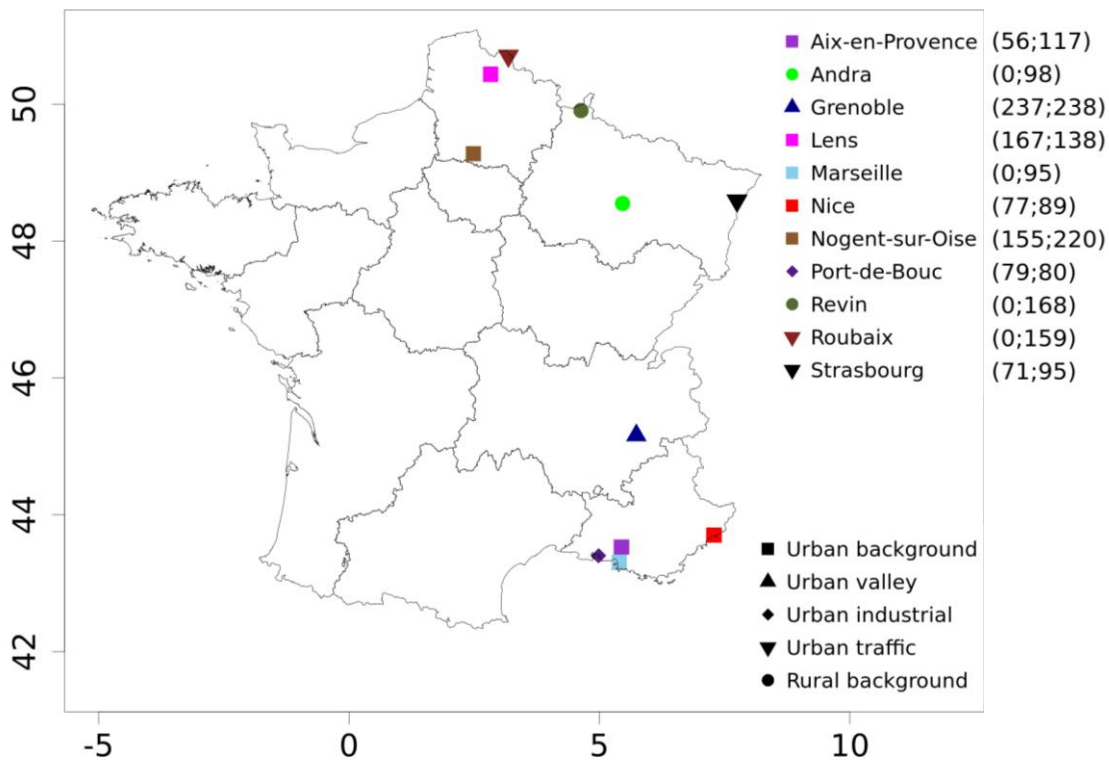


Figure 1 : Location and type of sites for PM₁₀ polyols measurements from filters as well as organic matter from the primary biogenic PMF factor (OMpb) over the years 2013 and 2014. The number of daily data use at each site is given in brackets, starting with the number of data for OMpb and then for polyols.

202 Sites are distributed over different geographical areas (Figure 1) in in the
northeast and southeast of France, including cities from the Channel region (Lens,
204 Roubaix, Nogent sur Oise) to the German border (Strasbourg), remote rural sites
located in between (Revin and Andra-OPE) as well as sites an Alpine urban station
(Grenoble) and sites near the Mediterranean Sea (Aix-en-Provence, Marseille, Nice,
206 Port-de-Bouc). These sites are classified as rural background (Andra-OPE, Revin),
urban background (Aix-en-Provence, Grenoble, Lens, Marseille, Nogent-sur-Oise,
208 Nice, Petit Quevilly, Talence), traffic sites (Roubaix, Strasbourg), urban industrial (Port-
de-Bouc). It is thought that the varied characteristics of the observational sites can give
210 us an unprecedented possibility of evaluation of the simulated spore emissions and
concentrations.

212

2.2. Regional Modelling

214 2.2.1. The chemistry transport model CHIMERE

216 CHIMERE is an eulerian state-of-the-art regional chemistry transport model
(Menut et al., 2021). It is used operationally by the French platform PREV'AIR (Rouil
218 et al., 2009) and the Copernicus Atmospheric Modelling System (CAM5) (Marécal et
al., 2015) to forecast and monitor air quality. The version v2020r3 of CHIMERE has
220 been used in this work (Menut et al., 2021).

222 The EMEP anthropogenic emissions inventory with a resolution of 10 km²
provides input data for anthropogenic emissions based on the methodology described
in Vestreng (2003). Biogenic VOC emissions are computed by CHIMERE based on
224 the Model of Emissions and Gases and Aerosols from Nature MEGAN 2.1 algorithm
(Guenther et al., 2012). The gas phase chemistry is provided by the Melchior2
226 mechanism (Derognat et al., 2003). The ISORROPIA II thermodynamic model is used
to compute the formation of inorganic aerosols based on the approach described in
228 Fountoukis and Nenes (2007). For organic aerosol formation and volatilisation of
primary organic aerosol, the volatility basis set (VBS) for the organic species as
230 described in Cholakian et al. (2018) was activated.

232 Chemical boundary conditions with a 3-hour temporal resolution are from the
CAM5 project (Marécal et al., 2015), together with the chemical fields for the model
upper boundary at the 500 hPa level. The WRF 3.7.1 model (Skamarock et al., 2008)
234 is used for meteorological simulation coupled to CHIMERE with no aerosol effect. The
spectral nudging (Von Storch et al., 2000) is used with NCEP temperature, wind,
236 humidity, pressure for wavelengths higher than 2 000 km whereas in the boundary
layer the WRF model freely generates its own dynamic. For the emissions of biogenic
238 volatile organic compounds (VOC) as well as for the parameterisation of the emissions
of primary organic aerosols, we use the LAI (Leaf Area Index) obtained from the
240 observations of the MODIS instrument with a frequency of 8 hours and a native
resolution of 30 seconds for each year (Sindelarova et al., 2014). The simulation has
242 been carried out during years 2013 and 2014 on a Western European domain, with a
9 x 9 km² horizontal resolution without nesting. It is run on 9 vertical hybrid levels from
244 ground to an upper height of 500 hPa, the height of the first layer being around 20
meters.

246

248 2.2.2. Parameterisation of fungal spore OA emissions

250 In the Introduction section, we have presented several parameterisations of
251 fungal spores. Among the three of them (H&S, S&D and Hummel) compared by
252 Hummel et al. (2015) to observations, the S&D parameterisation showed the worst
253 statistical agreement, and also is based on seasonally fixed land-use parameters. It
254 was therefore discarded. Among the two better performing parameterisations, we
255 preferred the H&S parameterisation. This is because our tests over the summer of
256 2014 with the Hummel's approach show that the inclusion of a temperature-dependent
257 and vegetation-independent term leads to significant fungal spore emissions under
258 high temperature conditions even at places where LAI is small and therefore no large
259 emissions are expected (sea and oceans, arid and desert soils). Finally, two recent
260 parameterisations by Janssen et al. (2021) have been developed over the eastern
261 United States using measurements of spore concentrations consider LAI, specific
262 humidity and wind friction velocity in the first case, and a spore population model in the
263 second. Comparisons with annual measurements of fluorescent primary organic
264 aerosols at German, Finnish and Colorado sites show similar correlations between
265 these two parameterisations and that of H&S (Janssen et al., 2021). With respect to
266 these simulations, we preferred the simpler H&S parameterisation. This
267 parameterisation was integrated in our simulations for its robustness at different sites
268 and it has been set-up specifically for temperate latitude European conditions.

269 Equation 1 shows the fungal spore emission flux $F_{H\&S}$ (unit: number of spores
270 $m^{-2} s^{-1}$) varying as a function of leaf area index **LAI** and specific humidity q_v . The
271 constant c , equal to $2315 m^{-2} s^{-1}$, introduced by Hoose et al. (2010) accounts for fungal
272 spore emission fluxes with an aerodynamic diameter of $3 \mu m$ instead of $5 \mu m$ (which
273 was initially estimated).

$$274 F_{H\&S} = c \frac{LAI}{5 m^2 \cdot m^{-2}} \frac{q_v}{1.5 \times 10^{-2} kg \cdot kg^{-1}} = 30\ 867 \times LAI \times q_v \quad (1)$$

275

276

277

278 Fungal spore number concentrations are transformed into mass using an
279 aerosol relative density of $1 kg kg^{-1}$ which is used as reference relative density for the
280 definition of aerodynamic diameter. All mass is attributed to organic matter. Within
281 CHIMERE, fungal spores OA are prescribed as a new species considered as
282 chemically inert in our simulation, but they can influence the condensation of semi-
283 volatile secondary organic compounds (as part of the organic aerosol phase) and act
284 as cloud condensation nuclei (Patade et al., 2021). Fungal spores are treated as non-
285 soluble particles and considered as monodispersed with a diameter of $3 \mu m$ in a model
286 size class closest to $3 \mu m$. In the model configuration with 10 size bins, spores are
287 included in the size bin 8 corresponding to sizes between 2.5 and $5 \mu m$, with an
288 average diameter of $3.5 \mu m$. However, no conclusive laboratory data are available to
289 include such processes in a model. Other processes considered in the model apart
290 from emissions are transport, and size-resolved dry and wet deposition with
291 characteristics like that of primary anthropogenic aerosols.

292

3. Results

294

We will present here the results of the two-year long simulations containing fungal spores' organic aerosol. Our initial analysis delves into the variability of simulated emissions and concentration patterns, along with their impact on the simulated PM₁₀ levels. We will then present an assessment of the simulated concentration fields with respect to polyol observations as well as primary biogenic organic burden as determined by the source apportionment studies.

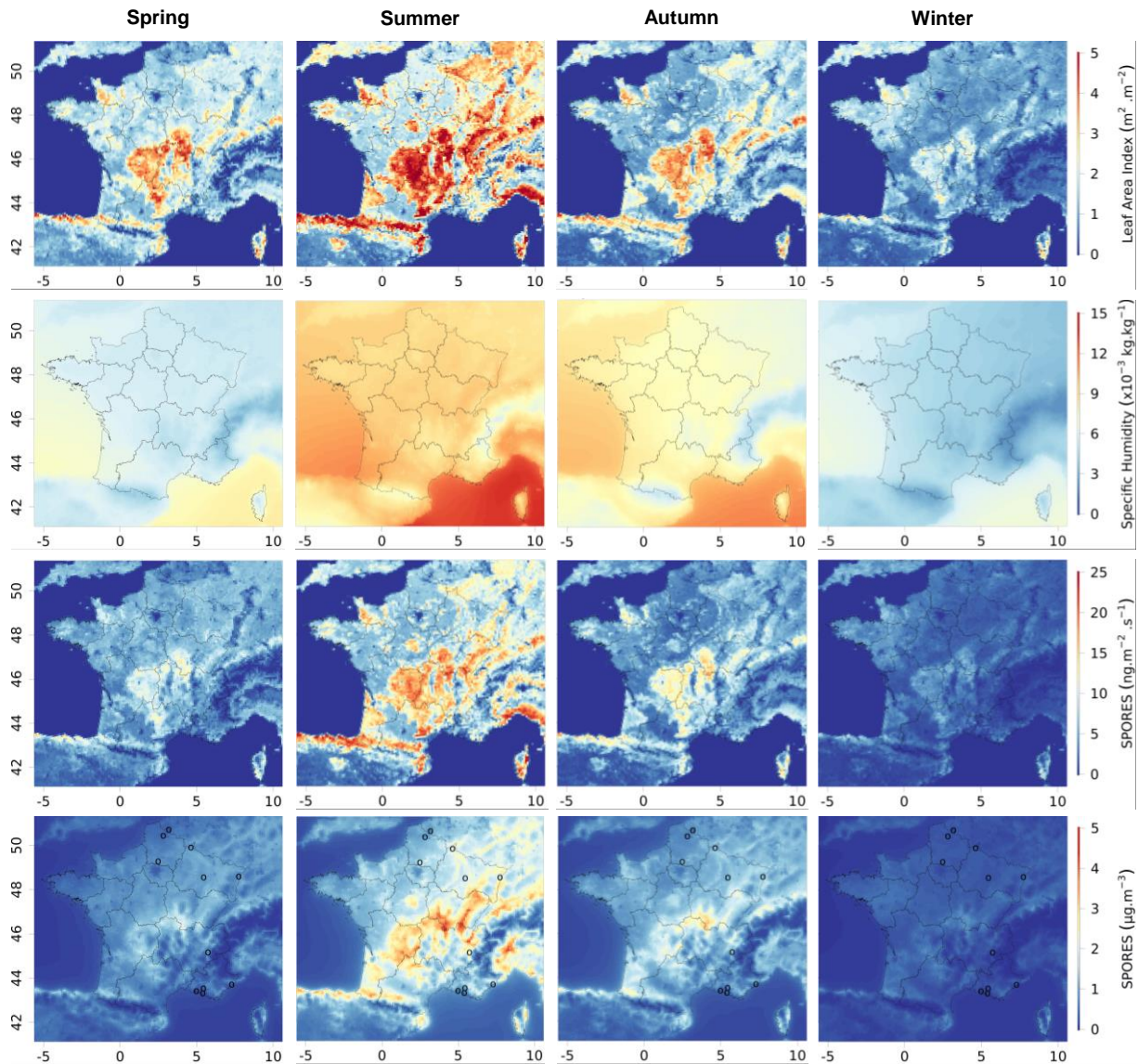
3.1. Simulated two years of fungal spore primary organic aerosol

Figure 2 presents the seasonal variation in emissions and concentrations of fungal spore primary organic aerosols for the years 2013 and 2014 averaged, as well as that of LAI and specific humidity, obtained from our simulations. As parametrised, emissions are largely driven by vegetation density (represented here by the LAI) with emission structures that follow the distribution of the main French forest areas. Major forested areas and emission hotspots are seen over the Massif Central (centred at 2 °E, 45.5 °N), the Jura (6 °E, 47 °N), the lower parts of the Alps (7 °E, 46 °N) and Pyrenees (0 °E, 43 °N), and the Landes Forest (-1 °W, 45 °N). Specific humidity, which is the other parameter used explicitly in the flux calculation (equation 1), is more homogeneous and its signature on the fluxes of spore emissions is less easily identifiable. LAI and specific humidity show the same seasonal cycles with higher values in summer and lower values in winter when the vegetation density and water content of the colder atmosphere are lowest. We can therefore hypothesise that LAI and specific humidity are responsible for much greater fungal spore emissions in summer than in winter.

Concentrations of atmospheric spores are found to be highly correlated with emissions, both spatially and on a seasonal scale. Small differences can be explained by transport and deposition processes. For instance, due to advection, contrasts in concentrations are less pronounced than those in emissions. Hummel et al. (2015) assumes that the lifetime of fungal spores is of about 5 hours in the atmospheric boundary layer. This short lifetime means that there is a small chance of long-distance transport, which explains the closeness of local concentrations to emission sources. Moreover, in our simulations, the total deposition flux of fungal spores is fairly rapid and can reach a maximum of 10 ng m⁻² s⁻¹ on average over the two years, with 8 ng m⁻² s⁻¹ for dry deposition and 5 ng m⁻² s⁻¹ for wet deposition. In summer, this total spore deposition reaches a maximum of 20 ng m⁻² s⁻¹ in France, around 12 ng m⁻² s⁻¹ in the Massif Central, while spore emissions peak in this area at 25 ng m⁻² s⁻¹ on average over the summer period. The difference in emissions and deposition is therefore significant, confirming also partial transport out of source regions. Since only the transport and deposition of fungal spores are taken into account, without interactions with other species, the conditions are similar to those of Hummel et al. (2015), with a lifetime of the same order of magnitude (5 hours), further confirming the low transport of spores.

Despite these conditions of transport and deposition, spore concentrations at locations up to a few hundred kilometers away can be similar in mass and temporal variation, explained by similar meteorological conditions and leaf area index, leading

340 to simultaneous emissions (Samaké et al., 2019b). Seasonal averages of fungal spore
342 concentrations can reach values of several $\mu\text{g m}^{-3}$ over large geographical areas,
344 especially over the forested areas in the southern part of France (Massif Central). This
346 is significant in view of the PM_{10} concentration there and consistent with previous
348 studies (Heald and Spracklen, 2009). For instance, fungal spore OA contributes to
350 about 20 % of PM_{10} mass on summer averaged over the Massif Central (Figure 3). On
352 the contrary, during winter, fungal spore concentrations remain always below $0.5 \mu\text{g m}^{-3}$,
354 and do not contribute much to PM_{10} , with a value always below a few percent.
356 Spring and autumn are intermediate, both in terms of fungal spore OA concentrations
358 and contributions to PM_{10} . With the lower formation of BSOA compared to summer,
360 the contribution of fungal spores to OM is largest in autumn, when it can reach around
40 %. It can reach about 30 % in other seasons with some geographical disparities.
Despite low emissions and concentrations, the contributions of spores to
concentrations of biogenic organic aerosols (BOA) is greatest in winter, reaching up to
70 %, due to the very low contribution of secondary biogenic organic aerosols during
this period, in contrast to the summer period.



362

Figure 2 : Seasonal mean leaf area index (LAI), specific humidity, as well as emissions and concentrations of fungal spores modelled with CHIMERE for 2013 and 2014 in France, respectively from top to bottom. The seasonal variation for spring (March to May), summer (June to August), autumn (September to November), and winter (December to February), are illustrated respectively from left to right. The circles represent the location of the measurement sites. The same maps are shown in the supplement (Figure S1).

364

366

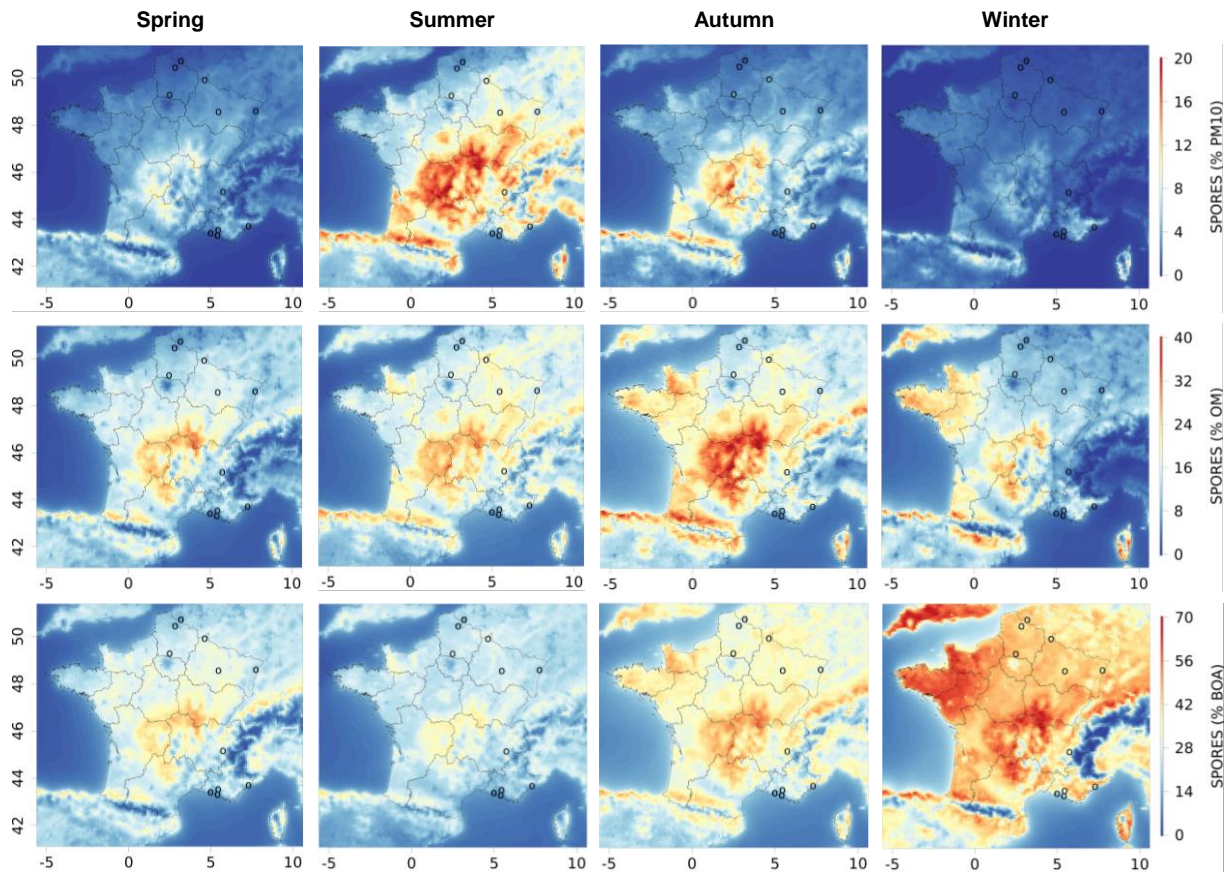
368

370

372

374

376



380 **Figure 3 : Seasonal contribution of fungal spores organic aerosols to PM₁₀, OM and biogenic organic**
 382 **aerosols (BOA) modelled with CHIMERE for 2013 and 2014 in France, respectively from top to bottom. The**
 seasonal variation for spring (March to May), summer (June to August), autumn (September to November),
 and winter (December to February), are illustrated respectively from left to right. The circles represent the
 location of the measurement sites. The same maps are shown in the supplement (Figure S2).

384

386

3.2. Comparison of fungal spore simulations to observations

388 3.2.1. General comparison for the entire data set

390 In order to compare simulations with observations, we can rely on two types of
 392 datasets available for several sites (as described respectively in sections 2.1.1 and
 2.1.2): first the polyol concentrations, and second the total OM concentration within the
 394 primary biogenic factor (OM_{pb}) derived from PMF analysis of PM₁₀ filter samples. For
 these comparisons to be meaningful, we need to convert the simulated fungal spore
 396 organic aerosol concentrations into polyol ones. Bauer et al. (2008b) derived a
 conversion factor for this purpose, for the temperate latitude continental urban site of
 398 Vienna. For the sum of arabitol and mannitol, which are the two sugar alcohol species
 measured in our data base, the latter authors found an average mass of 2.9 (2 – 4.2)
 400 pg per fungal spore. Elbert et al. (2007) assumed an average mass of a fungal spore
 of 65 pg. Combining these values yields to a percentage of polyol per mass of fungal
 spore of 4.5 % (3.1 – 6.5 %), which will be used for the comparisons that follow. This

402 is coherent with the work of Heald and Spracklen (2009), who used this same
 404 combination of values in order to derive their initial estimation of the mass of fungal
 spore emissions from multi-site polyol measurements.

We can first obtain a general picture of the performances of the model by
 406 studying the correlations and biases for all of sites with polyol measurements. For the
 169 polyol monthly averages from 11 sites, the median mean fractional bias (MFB) is
 408 slightly negative (-11 %), but with a large range of values for individual sites ranging
 from -78 % to +53 % (Figure 4, Table S1)¹. Using the lower and upper boundaries for
 410 the conversion factor between mass of spore and mass of polyols (3.1 and 6.5,
 respectively), the corresponding median MFB values would be -47 % and +26 %. As
 412 a conclusion, within the range of quantified uncertainties, the median MFB for monthly
 polyol means of -11 % is statistically close to zero. A bias calculation performed directly
 414 with the 1497 daily means shows very similar results, with a median MFB of -11 %
 (range for the -81 % to +49 %). This is not surprising, since the comparison of monthly
 416 means has been based only on days for which observations were available. The
 complicated results observed at stations on the Mediterranean coast (Aix-en-
 418 Provence, Marseille, Nice, Port-de-Bouc) will be discussed in the next section.

Next, simulated fungal spore OA is compared to OM in the primary biogenic
 420 factor (OMpb) (see section 2.1.2). Our simulations show a median bias (MFB) of -28
 % and a range from -116 % to +22 % for different sites (Figure 4, data from 98 monthly
 422 means for 7 sites). A negative bias is expected for this comparison, since the PMF
 factor is likely to include OM contributions from BSOA in addition to that from fungal
 424 spores (see section 2.1.2). As a result of this bias analysis with two different types of
 observations (polyols, OMpb), we do not observe the presence of a systematic bias for
 426 our fungal spore OA simulations for the ensemble of French sites. This agrees with
 (Hummel et al., 2015), who also could not conclude on a significant bias of the H&S
 428 parameterisation.

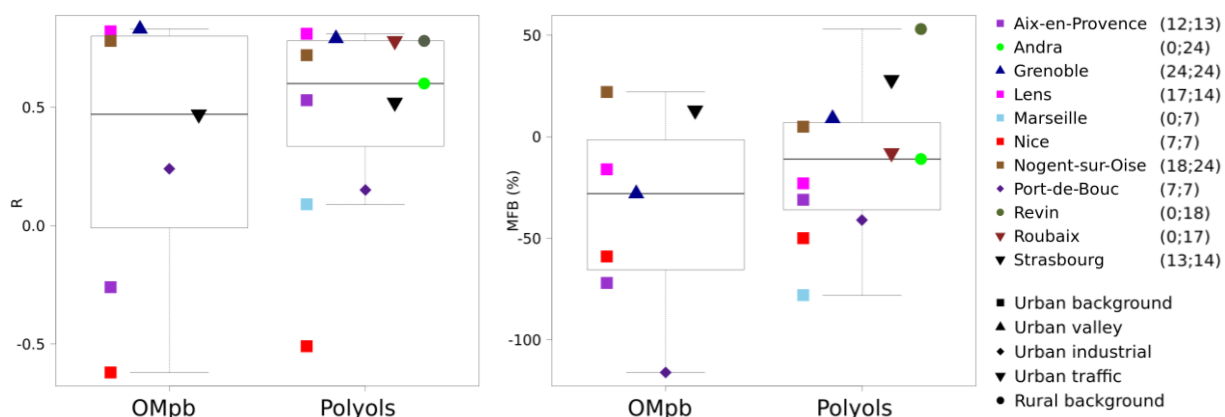


Figure 4 : Comparisons of simulated monthly mean concentrations of fungal spore OA to OM from PMF primary biogenic factor (OMpb) and polyols measurements (sum of mannitol and arabitol). Correlations and mean fractional bias (MFB) boxplots are obtained using the scores for each site (1 point per site) and are illustrated respectively at left and right side. The points corresponding to the sites represent the scores obtained on all the data for the site. Ranges between minimal and maximal values, and medians for respectively 7 and 11 sites. The number of monthly data for OMpb and polyols are noted next to the station list out of a total of respectively 98 and 169 monthly data. The same figure with daily data is shown in the supplement (Figure S3).

¹ Note that following the definition of MFB (see SI), a relative difference between simulations and observations of a factor 2 (1/2) corresponds to a MFB of 67 % (-67 %). Thus in very crude manner, the simulations with sites with the largest and lowest MFB show a factor 2 difference with observations.

430 The data sets were also used in order to assess if the H&S parameterisation is
432 able to reproduce the daily and the monthly average time variation (Figure 4 and Figure
434 S3, Table S1). For daily polyol averages, the median correlation between simulations
436 and measurements is 0.43 with a range from -0.19 to 0.57 for the 11 sites. The median
438 correlation is increased to 0.60 when looking at monthly averages with a large range
440 from -0.51 to 0.83. Expectedly, for many, but not all sites, the parameterisation better
442 depicts the seasonal variation (with larger summer and lower winter values) compared
to the daily variations (Figure S3). We will discuss this result further on a site-by-site
basis in section 3.2.2. Finally, for comparison with the same polyol data set, daily and
monthly mean fractional bias (MFB) are respectively -11 % and -11 % at all sites (Table
S1, Figure S3). The root mean square error (RMSE) and the mean fractional error
(MFE) was also calculated for estimating the error (Table S1, Figure S4). Daily and
monthly MFE are respectively 79 % and 56 % at all sites; for the median RMSE the
results are respectively $0.04 \mu\text{g m}^{-3}$ and $0.03 \mu\text{g m}^{-3}$.

444 3.2.2. Comparison of time series at selected sites

446 In this section, we evaluate the robustness of our simulations as a function of
448 the period of the year. To do so, comparisons are conducted between model outputs
450 and polyol observations, which are available for more measurement sites than sites
452 with PMF results. These comparisons especially aim at understanding the large ranges
454 of biases and correlations encountered in the previous section. Figure 5 shows
456 observed and estimated monthly mean polyol (sum of arabitol and mannitol
458 concentrations) at the sites with the most data (> 130 daily data) during years 2013
and 2014, namely Grenoble, Lens, Nogent-sur-Oise, Revin and Roubaix. These sites
also have the advantage of being of different types, respectively urban background in
an Alpine valley, urban background, urban background, rural background, and road
traffic. The time series for the other sites are shown in Figure S5, Figure S6, Figure
S7. We indicate both the simulated monthly means using data from all days, and only
for days for which filter samples are available.

Differences between simulations and measurements are small (<10 %) for most
460 of the values, which underlines the robustness of the model for monthly averages.
462 Figure 5 shows simulated seasonal cycles coherent with that in Figure 2 which reflects
464 the dependence of the simulated emissions on the LAI. We observe the maximum
466 monthly values for the summer months with a difference in structure between 2013
468 and 2014: while in 2013 the simulated maximum occurs in July for all of the sites, in
2014, it occurs in September at least for the sites in Northern France (Roubaix, Lens,
470 Nogent-sur-Oise, Andra-OPE, Strasbourg). The highest summer measurement values
472 of polyols ($0.1 - 0.15 \mu\text{g m}^{-3}$ corresponding to $2 - 3 \mu\text{g m}^{-3}$ of OMPb for monthly
474 averages) are of course simulated on the sites where the regional LAI are the strongest
(e.g. Grenoble, Andra-OPE, Revin, Strasbourg, Nogent-sur-Oise) as opposed to Lens,
Roubaix, Marseille, Aix, Port-de-Bouc for which the LAI of the adjacent regions are
lower. However, none of the measurement sites are located within the area of large
simulated fungal spore OA concentrations over the Massif Central. Comparisons
between simulations and observations show a remarkable agreement especially in the
seasonal variation for the stations in the northern part of France (Lens, Roubaix, Revin,
Nogent-sur-Oise), resulting in monthly correlation coefficients (R) of respectively 0.78,

476 0.83, 0.78 and 0.72. Specifically, the gradual increase in polyols (and related fungal
spores OM) from March to July is very well simulated, except for Revin for which
478 summer concentrations are overestimated. MFB values vary between -23 % for Lens
and +53 % for Revin.

480 Correlations for eastern French sites are a bit lower, with 0.60 for the Andra-
OPE site and 0.52 for Strasbourg with MFB respectively of -11 % and +28 %. For
482 Grenoble, a city in SE of France within the Alps, the correlation is good ($R = 0.79$) and
the bias is small (MFB = +9 %). For a group of sites in the south of France (Port-de-
484 Bouc, Marseille, Nice), located less than 10 km from the Mediterranean Sea, the
situation is singularly different, with strong underestimations in the simulation. It should
486 also be noted that we have fewer observations at these sites (only seven monthly mean
observations from June to December 2014), meaning that a full seasonal cycle was
488 not obtained. Still, the simulated decline in autumn/winter (October to December)
compared with summer (June to August) is not observed at these sites, resulting in low
490 or even negative correlations for monthly means between -0.51 and 0.15 and negative
biases (MFB values between -41 % and -78 %). Similarly, for Aix-en-Provence, some
492 30 km inland, winter polyol levels are strongly underestimated, resulting in a MFB of -
31 % and a correlation of 0.53.

494

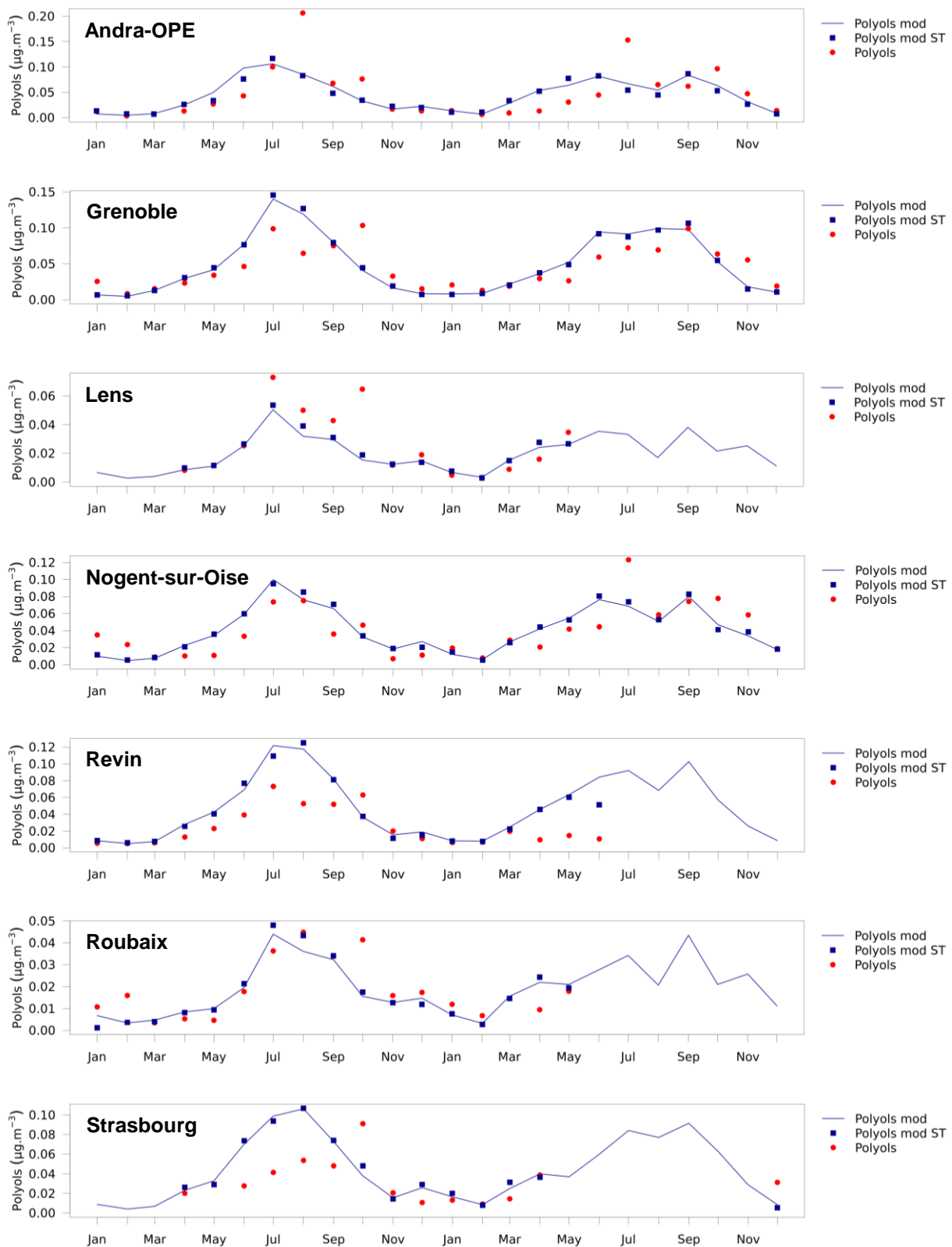


Figure 5 : Timeseries of monthly-mean polyol concentrations over 2013 and 2014 modelled by CHIMERE (blue line), measured at the sites (red dots) and modelled by CHIMERE using the same timebase as the measurements (blue squares). The simulated polyols values have been obtained by multiplying spore concentrations from CHIMERE by 4.5 %. Only the sites outside the Mediterranean area are shown. The same figures for Ompb and other sites are shown in the supplement (Figure S5, S6, S7).

496 3.3. Discussions

498 Overall, results obtained in this study demonstrate that the H&S
parameterisation implemented into the CHIMERE model works remarkably well to
500 reproduce the concentrations of fungal spore OA (or at least a proxy of these
concentrations, with the polyols measurements) observed at sites located in the
502 northern (Lens, Roubaix, Revin, Nogent-sur-Oise) and eastern (Andra-OPE,
Strasbourg, Grenoble) parts of France. Indeed, the seasonal cycles observed at these
504 sites and the intensity of the concentrations are remarkably well simulated by the model
for the monthly averages. This gives great confidence in the ability of the H&S
506 parameterisation to reproduce the fungal spore OA source over large parts of France.
This extends the results from the earlier work of Hummel et al. (2015) based on an
508 evaluation of 4 sites located in more northerly parts of Europe (Finland, Ireland, UK,
Germany) limited to a week in the end of August, to more southerly regions, but still
510 with temperate vegetation, and full seasonal cycles. For Europe, this extends also the
results from Janssen et al. (2021) who implemented the H&S parameterisation into
512 the global GEOS-Chem model. They compared the model output to yearly FBAP
observations at the same sites in Finland and Germany and found rather similar
514 seasonal variations with summer maxima and winter minima, although the simulated
maximum occurred in June (2010), while it was observed in August. Note that Janssen
516 et al. (2021) shows that the H&S parameterisation shows a strong overestimation of
fungal spore numbers with respect to observations in the US.

518 Another remarkable fact is that positive results in our study have been obtained
from sites with very different land-use typologies, ranging from traffic (Roubaix and
520 Strasbourg) and urban background (Lens, Nogent-sur-Oise) to rural (Revin, Andra-
OPE), or an urban background site within an Alpine valley (Grenoble). This can be
522 explained by the fact that, due to low levels of long-distance transport, fungal spore
OA seems to be controlled by the vegetation at local scale, as also pointed out already
524 for Grenoble by Samaké et al. (2019a).

526 Despite these overall encouraging results, several limitations appear for our
study. One is probably related to the simplification of using a unique LAI parameter
528 which cannot consider differences in vegetation typology. This may explain strong
differences in MFB values between sites in NE France: Revin, located in a forest rich
530 area in the Ardennes, shows a strong positive MFB of +53 % (the largest one
encountered in our study), while the Andra-OPE site surrounded by extensive field
532 crops shows an MFB of -11 %. For this latter site, we also can note that several
observed daily peaks (in August 2013 and July 2014), as large as $5 \mu\text{g m}^{-3}$ are not
534 simulated. Such peaks may be related to agricultural activities such as harvesting as
demonstrated by Samaké et al. (2019b) from the record of field work. In addition,
536 atmospheric concentrations of fungal spores mainly come from plant host species
(Samaké et al., 2020), so mechanised crop pruning and harvesting can have an impact
538 on spore concentrations in rural areas. The processes which are known to trigger
fungal spore emissions are not included specifically in the H&S parameterisation. In
540 the context of this work, we did not seek to better characterise this potential missing
source, but it is an interesting perspective for future work.

542 Our study also clearly shows the inability of the H&S parameterisation to
correctly reproduce OMpb and polyol measurements for Mediterranean areas in

544 Southern France, even though as noted before, our observational data base is weaker
546 for this region. However, at these sites, analysis of the chemical composition of
548 aerosols in the PM₁₀ fraction also showed poor simulation of the chemical species,
550 suggesting a more global problem in the Mediterranean area. This could be explained
552 by the specific dynamics in this sector (sea breezes, strong mistral-type winds) coupled
554 with significant orography and heavy urbanisation. As a result, failure to take account
556 of wind speed in the parameterisation of H&S may be a major cause of a lack of
558 emission and concentration in the Mediterranean area. Again, this failure may also be
560 related to the fact the LAI does not capture specific characteristics of Mediterranean
562 type vegetation, and which are not included in the H&S parameterisation, mainly tested
564 for sites mostly in northern Europe. In addition, it is striking that our simulations on
566 Mediterranean sites, as expected still simulate weak autumn/winter emissions due to
low LAI and specific humidity, but which are in contradiction to the still large observed
concentrations. This could be due to a relatively stronger importance of soil related
fungal spore emissions, which would be independent of LAI. Further, the drier and
hotter Mediterranean climate could lead to relatively smaller emissions during dry
summers and relatively larger emissions during winter still warm enough to allow for
fungal spore emissions. It was observed by Samaké et al. (2019b) that the sudden
and large decrease of the fall concentrations to the winter levels observed
simultaneously in Grenoble and Chamonix (160 km apart) coincides with a first night
temperature below +5 °C, which may be a threshold for the fungi population in this
area. Such complex relationships would not be captured by the single specific humidity
parameter which agglomerates information from relative humidity and temperature.

568 Finally, it may be noted that marine sources could also contribute to enhanced
570 polyol levels and organic aerosol at near coastal sites, although such sources are not
572 considered in our simulation. For instance, Fu et al. (2013) reports that large mannitol
574 concentrations, up to more than 50 ng m⁻³ over the Arctic Ocean, are comparable to
576 the maximum concentrations observed at our Mediterranean coastal sites. They
578 attribute this source to long range transport of fungal spores, despite the small
580 transport distance at least in the boundary layer due to efficient dry deposition. Direct
marine sources for polyols are an alternative explanation (algae, marine fungi).
Particularly, mannitol can account up to 20-30 % of the dry weight of some algae
species and is likely to be an important source of carbon for marine heterotrophic
bacteria (Groissillier et al., 2015). As a conclusion, the H&S parameterisation should not
be applied for PBOA emissions in Mediterranean or marine areas, and further work is
needed to better document PBOA concentrations and emission processes in such
areas.

582 4. Conclusions

584 In this work, we introduced the parameterisation proposed by Heald and
586 Spracklen (2009) for fungal spore OA emissions and updated by Hoose et al. (2010)
588 into the CHIMERE regional chemistry-transport model (hereafter called H&S). The
590 rationale for this work is to recognise the potentially important contribution of fungal
spore to summertime PM₁₀ (Samaké et al., 2019a, b) that can fill in the missing part of
the OM in chemistry transport models. The simplicity of the H&S parameterisation
gives us specific advantages: a unique LAI parameter gives a slow varying emission

592 potential, which is modulated with respect to meteorological conditions by specific
594 humidity.

596 Here, we largely extend the geographical and temporal validity of this
598 parameterisation, which has only been tested before for a limited dataset of
600 observations at northern European locations during the end of summer, to a two-year
602 dataset of seven sites over north-eastern France. Both polyols (more precisely sum of
604 arabitol and mannitol observations), and a primary biogenic organic aerosol factor from
PMF analysis show only limited biases for these sites, respectively +5 % and -2 %, in
terms of MFB (from 4 sites only for the comparison with PMF analysis). These small
biases, largely within the incertitude of the polyol/OM conversion factor and of the PMF
factor, are a positive outcome of our study. In addition, for this group of sites, the
seasonal variation of fungal spore emissions, displaying large summer and small
winter values, is correctly depicted, as manifested in large monthly mean correlations
(median 0.78, range from 0.52 to 0.83, from polyol measurements).

606 Still, and obviously, limitations can be noted, such as a wide range of biases for
608 individual sites, with MFB values between -23 % and +53 % for polyol observations.
610 This might be related to biome specific differences in the emissions only described by
612 a single LAI parameter. The emission variability on a day-to-day basis is only partly
614 expressed by the single specific humidity parameter (range of correlation coefficients
616 between 0.31 and 0.57 for the polyol measurements at the 7 sites in North-eastern
France). Here, using a more sophisticated combination of meteorological parameters
would be desirable to improve the modelling, as for example in Janssen et al. (2021)
including also maximum and minimum daily temperatures and friction velocity (even if
these authors did not evaluate the capacity of such a combination to simulate the daily
PBOA variation). One possible reason for the lack of correlation in daily time series is
the impact of land-use dependent activities, such as annual harvest or tilling in
agricultural areas.

618 For a smaller group of Mediterranean sites, with less observational data
620 coverage, the H&S parameterisation failed to capture fungal spore emissions both in
622 terms of absolute values and in seasonal variations, leading to strong negative biases
624 especially during the autumn/winter seasons. As a conclusion, for this region the use
626 of the H&S parameterisation in regional PM modelling may not consider certain factors
628 necessary for these specific sites. In particular, the night-time temperature was milder
630 than at the other sites, allowing fungal spores to be released even in winter. Additional
efforts are required to enhance the model dynamics specifically over Mediterranean
coastal environment. This includes extending the simulation of fungal spores over
more extended periods in these locations which also includes an assessment of
transport and storage. Furthermore, there is a need to better characterise a source of
Mediterranean marine organic aerosol (AO) that is distinct from fungal spores but
shares the emission of polyols. It is also necessary to have more measurement points
in this specific area to be able to achieve a more concrete conclusion.

632 These two year-round CHIMERE simulations incorporating the H&S
634 parameterisation revealed a significant contribution of fungal spore OA to PM_{10} mass,
636 which is of the order of one percent or less during winter, and up to 20 % during
638 summer in high emission zones over forested areas such as the Massif Central. In
terms of contribution to OM, the simulated autumn fungal spore contribution is even as
high as 40 %. This large predicted fungal spore OA contribution over the Massif Central
however still warrants confirmation by observations.

640 Finally, the projected impact of fungal spore organic aerosol suggests significant
and seasonally variable contributions to both PM₁₀ and OM mass. Consequently, the
642 simulation of spores should be included in state-of-the-art chemistry transport models.
While the validity of the H&S parameterisation has been demonstrated with a good
644 agreement with measurements across northern and eastern France, its application is
cautioned against in Mediterranean regions.

646

Code and data availability

648 All measurement and PMF data for this paper are archived at the IGE, and are
available on request from the corresponding authors (JLJ and GU). The codes and
650 modelling data are available from the LISA authors (MV, GF, MB, GS).
The model is available here: <https://www.lmd.polytechnique.fr/chimere/>
652 The MODIS observations are available here :
<https://modis.gsfc.nasa.gov/data/dataproduct/mod15.ph>

654

Author contributions

JLJ and GU provided the PM₁₀, polyol and PMF speciation data developed at the IGE
658 for the PhD work of Abdoulaye Samaké and Samuel Weber. OF completed the data
set with those obtained at the LCSQA during the CARA programme. FC developed the
660 H&S parameterisation code at INERIS, GS adapted the code for a more recent version
of the CHIMERE model at LISA. AC contributed to the LAI mapping. MV, GF, MB,
662 designed the numerical experiments. MV performed the simulations, produced figures
and tables, and wrote the paper. All co-authors contributed to the discussion of the
664 results. MV prepared the paper with contributions from all co-authors. MV, MB, GF,
GS, JLJ and GU designed the study. MV, MB, GF, GS, JLJ, GU, OF, FC and AC
666 contributed to the writing of the article.

668

Competing interests

670 The authors declare that they have no conflict of interest.

672

Acknowledgments

674 This work was granted access to the HPC resources of TGCC under the
allocation 2022-A0130107232 made by GENCI.

676 The authors warmly thank the dedicated work of many personal in the field for
collecting the samples in all the sites from the AASQA (Atmo AuRA, Atmo Sud, Atmo
678 HdF, Atmo GE, ...). Also we would like to thank all the technicians in the Air O Sol
analytical plateau at IGE for their work on the samples.

680 Many thanks to Hans Puxbaum for a close look at the paper in ACPD and a few
interesting remarks. Thanks also to the 2 anonymous reviewers who helped to improve
682 the quality of this work.

684

686 **Financial support**

688 The PhD of M. V is funded by ADEME and the Paris Region in the framework of the
research network on air quality, the DIM Qi². This work has been supported by the EU
Horizon 2020 Green Deal project RI-URBANS (grant no. 101036245).

690 The ANR program “Atmospheric Biogenic Sugar” ANR-21-CE01-0021-01 provided
some financial support for this collaboration, while analytical aspects were also
692 supported at IGE by the Air-O-Sol platform within Labex OSUG@2020 (ANR10
LABX56). The work at IGE for the Andra-OPE site is supported by a long-term grant
694 from ANDRA.

696 **References**

Bauer, H., Kasper-Giebl, A., Löflund, M., Giebl, H., Hitzenberger, R., Zibuschka, F.,
698 and Puxbaum, H.: The contribution of bacteria and fungal spores to the organic carbon
content of cloud water, precipitation and aerosols, *Atmospheric Res.*, 64, 109–119,
700 [https://doi.org/10.1016/S0169-8095\(02\)00084-4](https://doi.org/10.1016/S0169-8095(02)00084-4), 2002.

Bauer, H., Claeys, M., Vermeylen, R., Schueller, E., Weinke, G., Berger, A., and
702 Puxbaum, H.: Arabitol and mannitol as tracers for the quantification of airborne fungal
spores, *Atmos. Environ.*, 42, 588–593,
704 <https://doi.org/10.1016/j.atmosenv.2007.10.013>, 2008a.

Bauer, H., Schueller, E., Weinke, G., Berger, A., Hitzenberger, R., Marr, I. L., and
706 Puxbaum, H.: Significant contributions of fungal spores to the organic carbon and to
the aerosol mass balance of the urban atmospheric aerosol, *Atmos. Environ.*, 42,
708 5542–5549, <https://doi.org/10.1016/j.atmosenv.2008.03.019>, 2008b.

Belis, C. A., Pernigotti, D., Pirovano, G., Favez, O., Jaffrezo, J. L., Kuenen, J., Denier
710 Van Der Gon, H., Reizer, M., Riffault, V., Alleman, L. Y., Almeida, M., Amato, F.,
Angyal, A., Argyropoulos, G., Bande, S., Beslic, I., Besombes, J.-L., Bove, M. C.,
712 Brotto, P., Calori, G., Cesari, D., Colombi, C., Contini, D., De Gennaro, G., Di Gilio, A.,
Diapouli, E., El Haddad, I., Elbern, H., Eleftheriadis, K., Ferreira, J., Vivanco, M. G.,
714 Gilardoni, S., Golly, B., Hellebust, S., Hopke, P. K., Izadmanesh, Y., Jorquera, H.,
Krajsek, K., Kranenburg, R., Lazzeri, P., Lenartz, F., Lucarelli, F., Maciejewska, K.,
716 Manders, A., Manousakas, M., Masiol, M., Mircea, M., Mooibroek, D., Nava, S.,
Oliveira, D., Paglione, M., Pandolfi, M., Perrone, M., Petralia, E., Pietrodangelo, A.,
718 Pillon, S., Pokorna, P., Prati, P., Salameh, D., Samara, C., Samek, L., Saraga, D.,
Sauvage, S., Schaap, M., Scotto, F., Sega, K., Siour, G., Tauler, R., Valli, G., Vecchi,
720 R., Venturini, E., Vestenius, M., Waked, A., and Yubero, E.: Evaluation of receptor and
chemical transport models for PM₁₀ source apportionment, *Atmospheric Environ. X*,
722 5, 100053, <https://doi.org/10.1016/j.aeaoa.2019.100053>, 2020.

Borlaza, L. J. S., Weber, S., Uzu, G., Jacob, V., Cañete, T., Micallef, S., Trébuchon,
724 C., Slama, R., Favez, O., and Jaffrezo, J.-L.: Disparities in particulate matter (PM₁₀)
origins and oxidative potential at a city scale (Grenoble, France) – Part 1: Source
726 apportionment at three neighbouring sites, *Atmospheric Chem. Phys.*, 21, 5415–5437,
<https://doi.org/10.5194/acp-21-5415-2021>, 2021.

- 728 Cavalli, F., Viana, M., Yttri, K. E., and Genberg, J.: Toward a standardised thermal-
730 optical protocol for measuring atmospheric organic and elemental carbon: the
EUSAAR protocol, *Atmospheric Meas. Tech.*, 3, 79–89, <https://doi.org/10.5194/amt-3-79-2010>, 2010.
- 732 Cholakian, A., Beekmann, M., Colette, A., Coll, I., Siour, G., Sciare, J., Marchand, N.,
734 Couvidat, F., Pey, J., Gros, V., Sauvage, S., Michoud, V., Sellegri, K., Colomb, A.,
Sartelet, K., Langley DeWitt, H., Elser, M., Prévot, A. S. H., Szidat, S., and Dulac, F.:
736 Simulation of fine organic aerosols in the western Mediterranean area during the
ChArMEx 2013 summer campaign, *Atmospheric Chem. Phys.*, 18, 7287–7312,
<https://doi.org/10.5194/acp-18-7287-2018>, 2018.
- 738 Derognat, C., Beekmann, M., Baeumle, M., Martin, D., and Schmidt, H.: Effect of
740 biogenic volatile organic compound emissions on tropospheric chemistry during the
Atmospheric Pollution Over the Paris Area (ESQUIF) campaign in the Ile- de- France
742 region, *J. Geophys. Res. Atmospheres*, 108, 8560,
<https://doi.org/10.1029/2001JD001421>, 2003.
- 744 Després, V. R., Huffman, J. A., Burrows, S. M., Hoose, C., Safatov, A. S., Buryak, G.,
Fröhlich-Nowoisky, J., Elbert, W., Andreae, M. O., Pöschl, U., and Jaenicke, R.:
746 Primary biological aerosol particles in the atmosphere: a review, *Tellus B Chem. Phys.
Meteorol.*, 64, 15598, <https://doi.org/10.3402/tellusb.v64i0.15598>, 2012.
- 748 Douwes, J., Thorne, P., Pearce, N., and Heederik, D.: Bioaerosol Health Effects and
Exposure Assessment: Progress and Prospects, *Ann. Occup. Hyg.*, 47, 187–200,
<https://doi.org/10.1093/annhyg/meg032>, 2003.
- 750 Eduard, W., Heederik, D., Duchaine, C., and Green, B. J.: Bioaerosol exposure
752 assessment in the workplace: the past, present and recent advances, *J. Environ.
Monit.*, 14, 334, <https://doi.org/10.1039/c2em10717a>, 2012.
- 754 Elbert, W., Taylor, P. E., Andreae, M. O., and Pöschl, U.: Contribution of fungi to
primary biogenic aerosols in the atmosphere: wet and dry discharged spores,
756 carbohydrates, and inorganic ions, *Atmospheric Chem. Phys.*, 7, 4569–4588,
<https://doi.org/10.5194/acp-7-4569-2007>, 2007.
- 758 Favez, O., El Haddad, I., Piot, C., Boréave, A., Abidi, E., Marchand, N., Jaffrezo, J.-L.,
Besombes, J.-L., Personnaz, M.-B., Sciare, J., Wortham, H., George, C., and D’Anna,
760 B.: Inter-comparison of source apportionment models for the estimation of wood
burning aerosols during wintertime in an Alpine city (Grenoble, France), *Atmospheric
Chem. Phys.*, 10, 5295–5314, <https://doi.org/10.5194/acp-10-5295-2010>, 2010.
- 762 Favez, O., Weber, S., Petit, J.-E., Alleman, L. Y., Albinet, A., Riffault, V., Chazeau, B.,
764 Amodeo, T., Salameh, D., Zhang, Y., Srivastava, D., Samaké, A., Aujay-Plouzeau, R.,
Papin, A., Bonnaire, N., Boullanger, C., Chatain, M., Chevrier, F., Detournay, A.,
766 Dominik-Sègue, M., Falhun, R., Garbin, C., Ghersi, V., Grignion, G., Levigoureux, G.,
Pontet, S., Rangognio, J., Zhang, S., Besombes, J.-L., Conil, S., Uzu, G., Savarino, J.,
768 Marchand, N., Gros, V., Marchand, C., Jaffrezo, J.-L., and Leoz-Garziandia, E.:
Overview of the French Operational Network for In Situ Observation of PM Chemical
770 Composition and Sources in Urban Environments (CARA Program), *Atmosphere*, 12,
207, <https://doi.org/10.3390/atmos12020207>, 2021.

- 772 Fountoukis, C. and Nenes, A.: ISORROPIA II: a computationally efficient
thermodynamic equilibrium model for K^+ – Ca^{2+} – Mg^{2+} – NH_4^+ – Na^+ – SO_4^{2-} – NO_3^- –
Cl– H_2O aerosols, *Atmos Chem Phys*, 2007.
- 774 Fröhlich-Nowoisky, J., Kampf, C. J., Weber, B., Huffman, J. A., Pöhlker, C., Andreae,
M. O., Lang-Yona, N., Burrows, S. M., Gunthe, S. S., Elbert, W., Su, H., Hoor, P.,
776 Thines, E., Hoffmann, T., Després, V. R., and Pöschl, U.: Bioaerosols in the Earth
system: Climate, health, and ecosystem interactions, *Atmospheric Res.*, 182, 346–
778 376, <https://doi.org/10.1016/j.atmosres.2016.07.018>, 2016.
- 780 Fu, P. Q., Kawamura, K., Chen, J., Charrière, B., and Sempéré, R.: Organic molecular
composition of marine aerosols over the Arctic Ocean in summer: contributions of
primary emission and secondary aerosol formation, *Biogeosciences*, 10, 653–667,
782 <https://doi.org/10.5194/bg-10-653-2013>, 2013.
- 784 Ghosh, B., Lal, H., and Srivastava, A.: Review of bioaerosols in indoor environment
with special reference to sampling, analysis and control mechanisms, *Environ. Int.*, 85,
254–272, <https://doi.org/10.1016/j.envint.2015.09.018>, 2015.
- 786 Gosselin, M. I., Rathnayake, C. M., Crawford, I., Pöhlker, C., Fröhlich-Nowoisky, J.,
Schmer, B., Després, V. R., Engling, G., Gallagher, M., Stone, E., Pöschl, U., and
788 Huffman, J. A.: Fluorescent bioaerosol particle, molecular tracer, and fungal spore
concentrations during dry and rainy periods in a semi-arid forest, *Atmospheric Chem.*
790 *Phys.*, 16, 15165–15184, <https://doi.org/10.5194/acp-16-15165-2016>, 2016.
- 792 Groisillier, A., Labourel, A., Michel, G., and Tonon, T.: The Mannitol Utilization System
of the Marine Bacterium *Zobellia galactanivorans*, *Appl. Environ. Microbiol.*, 81, 1799–
1812, <https://doi.org/10.1128/AEM.02808-14>, 2015.
- 794 Guenther, A. B., Jiang, X., Heald, C. L., Sakulyanontvittaya, T., Duhl, T., Emmons, L.
K., and Wang, X.: The Model of Emissions of Gases and Aerosols from Nature version
796 2.1 (MEGAN2.1): an extended and updated framework for modeling biogenic
emissions, *Geosci. Model Dev.*, 5, 1471–1492, [https://doi.org/10.5194/gmd-5-1471-](https://doi.org/10.5194/gmd-5-1471-2012)
798 2012, 2012.
- 800 Heald, C. L. and Spracklen, D. V.: Atmospheric budget of primary biological aerosol
particles from fungal spores, *Geophys. Res. Lett.*, 36, 2009GL037493,
<https://doi.org/10.1029/2009GL037493>, 2009.
- 802 Hoose, C., Kristjánsson, J. E., and Burrows, S. M.: How important is biological ice
nucleation in clouds on a global scale?, *Environ. Res. Lett.*, 5, 024009,
804 <https://doi.org/10.1088/1748-9326/5/2/024009>, 2010.
- 806 Hopke, P. K., Dai, Q., Li, L., and Feng, Y.: Global review of recent source
apportionments for airborne particulate matter, *Sci. Total Environ.*, 740, 140091,
<https://doi.org/10.1016/j.scitotenv.2020.140091>, 2020.
- 808 Huffman, J. A., Prenni, A. J., DeMott, P. J., Pöhlker, C., Mason, R. H., Robinson, N.
H., Fröhlich-Nowoisky, J., Tobo, Y., Després, V. R., Garcia, E., Gochis, D. J., Harris,
810 E., Müller-Germann, I., Ruzene, C., Schmer, B., Sinha, B., Day, D. A., Andreae, M. O.,
Jimenez, J. L., Gallagher, M., Kreidenweis, S. M., Bertram, A. K., and Pöschl, U.: High
812 concentrations of biological aerosol particles and ice nuclei during and after rain,

- 814 Atmospheric Chem. Phys., 13, 6151–6164, <https://doi.org/10.5194/acp-13-6151-2013>,
2013.
- 816 Hummel, M., Hoose, C., Gallagher, M., Healy, D. A., Huffman, J. A., O'Connor, D.,
Pöschl, U., Pöhlker, C., Robinson, N. H., Schnaiter, M., Sodeau, J. R., Stengel, M.,
818 Toprak, E., and Vogel, H.: Regional-scale simulations of fungal spore aerosols using
an emission parameterization adapted to local measurements of fluorescent biological
820 aerosol particles, *Atmospheric Chem. Phys.*, 15, 6127–6146,
<https://doi.org/10.5194/acp-15-6127-2015>, 2015.
- 822 Jaenicke, R., Matthias-Maser, S., and Gruber, S.: Omnipresence of biological material
in the atmosphere, *Environ. Chem.*, 4, 217, <https://doi.org/10.1071/EN07021>, 2007.
- 824 Janssen, R. H. H., Heald, C. L., Steiner, A. L., Perring, A. E., Huffman, J. A., Robinson,
E. S., Twohy, C. H., and Ziemba, L. D.: Drivers of the fungal spore bioaerosol budget:
826 observational analysis and global modeling, *Atmospheric Chem. Phys.*, 21, 4381–
4401, <https://doi.org/10.5194/acp-21-4381-2021>, 2021.
- 828 Jones, A. M. and Harrison, R. M.: The effects of meteorological factors on atmospheric
bioaerosol concentrations, a review, *Sci. Total Environ.*, 326, 151–180,
<https://doi.org/10.1016/j.scitotenv.2003.11.021>, 2004.
- 830 Karagulian, F., Belis, C. A., Dora, C. F. C., Prüss-Ustün, A. M., Bonjour, S., Adair-
Rohani, H., and Amann, M.: Contributions to cities' ambient particulate matter (PM): A
832 systematic review of local source contributions at global level, *Atmos. Environ.*, 120,
475–483, <https://doi.org/10.1016/j.atmosenv.2015.08.087>, 2015.
- 834 Marécal, V., Peuch, V.-H., Andersson, C., Andersson, S., Arteta, J., Beekmann, M.,
Benedictow, A., Bergström, R., Bessagnet, B., Cansado, A., Chéroux, F., Colette, A.,
836 Coman, A., Curier, R. L., Denier Van Der Gon, H. A. C., Drouin, A., Elbern, H., Emili,
E., Engelen, R. J., Eskes, H. J., Foret, G., Friese, E., Gauss, M., Giannaros, C., Guth,
838 J., Joly, M., Jaumouillé, E., Josse, B., Kadygrov, N., Kaiser, J. W., Krajsek, K., Kuenen,
J., Kumar, U., Liora, N., Lopez, E., Malherbe, L., Martinez, I., Melas, D., Meleux, F.,
840 Menut, L., Moinat, P., Morales, T., Parmentier, J., Piacentini, A., Plu, M., Poupkou, A.,
Queguiner, S., Robertson, L., Rouil, L., Schaap, M., Segers, A., Sofiev, M., Tarasson,
842 L., Thomas, M., Timmermans, R., Valdebenito, Á., Van Velthoven, P., Van Versendaal,
R., Vira, J., and Ung, A.: A regional air quality forecasting system over Europe: the
844 MACC-II daily ensemble production, *Geosci. Model Dev.*, 8, 2777–2813,
<https://doi.org/10.5194/gmd-8-2777-2015>, 2015.
- 846 Menut, L., Bessagnet, B., Briant, R., Cholakian, A., Couvidat, F., Mailler, S., Pennel,
R., Siour, G., Tuccella, P., Turquety, S., and Valari, M.: The CHIMERE v2020r1 online
848 chemistry-transport model, *Geosci. Model Dev.*, 14, 6781–6811,
<https://doi.org/10.5194/gmd-14-6781-2021>, 2021.
- 850 Paatero, P. and Tapper, U.: Positive matrix factorization: A non-negative factor model
with optimal utilization of error estimates of data values, *Environmetrics*, 5, 111–126,
852 <https://doi.org/10.1002/env.3170050203>, 1994.
- 854 Patade, S., Phillips, V. T. J., Amato, P., Bingemer, H. G., Burrows, S. M., DeMott, P.
J., Goncalves, F. L. T., Knopf, D. A., Morris, C. E., Alwmark, C., Artaxo, P., Pöhlker,

- 856 C., Schrod, J., and Weber, B.: Empirical formulation for multiple groups of primary biological ice nucleating particles from field observations over Amazonia, *J. Atmospheric Sci.*, 78, 2195–2220, <https://doi.org/10.1175/JAS-D-20-0096.1>, 2021.
- 858 Pearson, C., Littlewood, E., Douglas, P., Robertson, S., Gant, T. W., and Hansell, A. L.: Exposures and Health Outcomes in Relation to Bioaerosol Emissions From Composting Facilities: A Systematic Review of Occupational and Community Studies, *J. Toxicol. Environ. Health Part B*, 18, 43–69, <https://doi.org/10.1080/10937404.2015.1009961>, 2015.
- 864 Petit, J.-E., Favez, O., Sciare, J., Crenn, V., Sarda-Estève, R., Bonnaire, N., Močnik, G., Dupont, J.-C., Haeffelin, M., and Leoz-Garziandia, E.: Two years of near real-time chemical composition of submicron aerosols in the region of Paris using an Aerosol Chemical Speciation Monitor (ACSM) and a multi-wavelength Aethalometer, *Atmospheric Chem. Phys.*, 15, 2985–3005, <https://doi.org/10.5194/acp-15-2985-2015>, 2015.
- 870 Rouil, L., Honoré, C., Vautard, R., Beekmann, M., Bessagnet, B., Malherbe, L., Meleux, F., Dufour, A., Elichegaray, C., Flaud, J.-M., Menut, L., Martin, D., Peuch, A., Peuch, V.-H., and Poisson, N.: Prev'air: An Operational Forecasting and Mapping System for Air Quality in Europe, *Bull. Am. Meteorol. Soc.*, 90, 73–84, <https://doi.org/10.1175/2008BAMS2390.1>, 2009.
- 874 Samaké, A., Uzu, G., Martins, J. M. F., Calas, A., Vince, E., Parat, S., and Jaffrezo, J. L.: The unexpected role of bioaerosols in the Oxidative Potential of PM, *Sci. Rep.*, 7, 10978, <https://doi.org/10.1038/s41598-017-11178-0>, 2017.
- 878 Samaké, A., Jaffrezo, J.-L., Favez, O., Weber, S., Jacob, V., Canete, T., Albinet, A., Charron, A., Riffault, V., Perdrix, E., Waked, A., Golly, B., Salameh, D., Chevrier, F., Oliveira, D. M., Besombes, J.-L., Martins, J. M. F., Bonnaire, N., Conil, S., Guillaud, G., Mesbah, B., Rocq, B., Robic, P.-Y., Hulin, A., Le Meur, S., Descheemaeker, M., Chretien, E., Marchand, N., and Uzu, G.: Arabitol, mannitol, and glucose as tracers of primary biogenic organic aerosol: the influence of environmental factors on ambient air concentrations and spatial distribution over France, *Atmospheric Chem. Phys.*, 19, 11013–11030, <https://doi.org/10.5194/acp-19-11013-2019>, 2019a.
- 888 Samaké, A., Jaffrezo, J.-L., Favez, O., Weber, S., Jacob, V., Albinet, A., Riffault, V., Perdrix, E., Waked, A., Golly, B., Salameh, D., Chevrier, F., Oliveira, D. M., Bonnaire, N., Besombes, J.-L., Martins, J. M. F., Conil, S., Guillaud, G., Mesbah, B., Rocq, B., Robic, P.-Y., Hulin, A., Le Meur, S., Descheemaeker, M., Chretien, E., Marchand, N., and Uzu, G.: Polyols and glucose particulate species as tracers of primary biogenic organic aerosols at 28 French sites, *Atmospheric Chem. Phys.*, 19, 3357–3374, <https://doi.org/10.5194/acp-19-3357-2019>, 2019b.
- 892 Samaké, A., Bonin, A., Jaffrezo, J.-L., Taberlet, P., Weber, S., Uzu, G., Jacob, V., Conil, S., and Martins, J. M. F.: High levels of primary biogenic organic aerosols are driven by only a few plant-associated microbial taxa, *Atmospheric Chem. Phys.*, 20, 5609–5628, <https://doi.org/10.5194/acp-20-5609-2020>, 2020.

- 896 Shaffer, B. T. and Lighthart, B.: Survey of Culturable Airborne Bacteria at Four Diverse
Locations in Oregon: Urban, Rural, Forest, and Coastal, *Microb. Ecol.*, 34, 167–177,
898 <https://doi.org/10.1007/s002489900046>, 1997.
- Sindelarova, K., Granier, C., Bouarar, I., Guenther, A., Tilmes, S., Stavrakou, T.,
900 Müller, J.-F., Kuhn, U., Stefani, P., and Knorr, W.: Global data set of biogenic VOC
emissions calculated by the MEGAN model over the last 30 years, *Atmospheric Chem.*
902 *Phys.*, 14, 9317–9341, <https://doi.org/10.5194/acp-14-9317-2014>, 2014.
- Skamarock, W. C., Klemp, J. B., Dudhia, J., Gill, D. O., Barker, D. M., Duda, M. G.,
904 Huang, X.-Y., Wang, W., and Powers, J. G.: A Description of the Advanced Research
WRF Version 3, National Center for Atmospheric Research Boulder, Colorado, USA,
906 2008.
- Verlhac, S., Favez, O., and Albinet, A.: Interlaboratory comparison organized for the
908 European laboratories involved in the analysis of levoglucosan and its isomers,
LCSQA, Verneuil-en-Halatte, 2013.
- 910 Vestreng, V.: Review and Revision, Emission Data Reported to CLRTAP, MSC-W
Status Report, Norwegian Meteorological Institute, Oslo, Norway, 2003.
- 912 Von Storch, H., Langenberg, H., and Feser, F.: A Spectral Nudging Technique for
Dynamical Downscaling Purposes, *Mon. Weather Rev.*, 128, 3664–3673,
914 [https://doi.org/10.1175/1520-0493\(2000\)128<3664:ASNTFD>2.0.CO;2](https://doi.org/10.1175/1520-0493(2000)128<3664:ASNTFD>2.0.CO;2), 2000.
- Waked, A., Favez, O., Alleman, L. Y., Piot, C., Petit, J.-E., Delaunay, T., Verlinden, E.,
916 Golly, B., Besombes, J.-L., Jaffrezo, J.-L., and Leoz-Garziandia, E.: Source
apportionment of PM₁₀ in a north-western Europe regional urban background site
918 (Lens, France) using positive matrix factorization and including primary biogenic
emissions, *Atmospheric Chem. Phys.*, 14, 3325–3346, [https://doi.org/10.5194/acp-14-](https://doi.org/10.5194/acp-14-3325-2014)
920 [3325-2014](https://doi.org/10.5194/acp-14-3325-2014), 2014.
- Weber, S., Uzu, G., Favez, O., Borlaza, L. J., Calas, A., Salameh, D., Chevrier, F.,
922 Allard, J., Besombes, J.-L., Albinet, A., Pontet, S., Mesbah, B., Gille, G., Zhang, S.,
Pallares, C., Leoz-Garziandia, E., and Jaffrezo, J.-L.: Source apportionment of
924 atmospheric PM₁₀ Oxidative Potential: synthesis of 15 year-round urban datasets in
France, *Atmospheric Chem. Phys.*, 21, 11353–11378, [https://doi.org/10.5194/acp-21-](https://doi.org/10.5194/acp-21-11353-2021)
926 [11353-2021](https://doi.org/10.5194/acp-21-11353-2021), 2021.
- Yttri, K. E., Schnelle-Kreis, J., Maenhaut, W., Abbaszade, G., Alves, C., Bjerke, A.,
928 Bonnier, N., Bossi, R., Claeys, M., Dye, C., Evtyugina, M., García-Gacio, D., Hillamo,
R., Hoffer, A., Hyder, M., Iinuma, Y., Jaffrezo, J.-L., Kasper-Giebl, A., Kiss, G., López-
930 Mahia, P. L., Pio, C., Piot, C., Ramirez-Santa-Cruz, C., Sciare, J., Teinilä, K.,
Vermeulen, R., Vicente, A., and Zimmermann, R.: An intercomparison study of
932 analytical methods used for quantification of levoglucosan in ambient aerosol filter
samples, *Atmospheric Meas. Tech.*, 8, 125–147, [https://doi.org/10.5194/amt-8-125-](https://doi.org/10.5194/amt-8-125-2015)
934 [2015](https://doi.org/10.5194/amt-8-125-2015), 2015.

936